Bacterial sirtuin CobB and PRPP synthase crosstalk in regulation of protein acetylation

Beata M. Walter[1], Joanna Morcinek-Orłowska[1], Aneta Szulc[1], Andrew L. Lovering[2], Manuel Banzhaf[2], Monika Glinkowska[1] ✉

1- Department of Bacterial Molecular Genetics, Faculty of Biology, University of Gdansk, Gdansk, Poland

2 - Institute of Microbiology & Infection and School of Biosciences, University of Birmingham, UK;

✉ - to whom correspondence should be addressed; monika.glinkowska@ug.edu.pl

Abstract

Protein lysine acetylation, regulates a wide range of cellular functions and is controlled by protein deacetylases called sirtuins. In eukaryotes, sirtuins activity is coupled to the spatiotemporally-controlled NAD+ level. However, regulation of the bacterial sirtuin CobB and its coupling to the NAD+ metabolism is not well understood. In this work we show that such coordination in *Escherichia coli* cells is achieved through a CobB interaction with PRPP synthase Prs, an enzyme necessary for NAD+ synthesis. Probing CobB protein-protein interactions, we demonstrate that it forms a stable complex with Prs. This assembly stimulates CobB deacetylase activity and partially protects it from inhibition by nicotinamide. We provide evidence that Prs acetylation is not necessary for CobB binding but affects the global acetylome and CobB activity *in vivo*. Consequently, we show that Prs acetylation status affects bacterial growth under different metabolic regimes. Therefore, we propose that CobB-Prs crosstalk orchestrates the NAD+ metabolism and protein acetylation in response to environmental cues.

Key words: Protein acetylation/ sirtuins/ NAD metabolism/ phosporibosyl pyrophosphate

Intoduction

Lysine acetylation is a post-translational protein modification regulating a wide range of protein functions. It has been investigated thoroughly in eukaryotic cells and recently was discovered to be important for protein regulation in prokaryotes as well (Bernal et al., 2014; Christensen et al., 2019). In bacteria, the level of protein acetylation is a result of two

counterbalancing processes. Proteins become acetylated enzymatically or chemically, by lysine transacetylases or acetyl phosphate, respectively (Kuhn et al., 2014; Ma and Wood, 2011; Weinert et al., 2013). In the opposing process, acetyl groups are removed from acetyl-lysine residues by deacetylases, most of which are NAD+-dependent homologs of eukaryotic sirtuins (Greiss and Gartner, 2009; Imai and Guarente, 2010).

CobB is a highly conserved protein lysine deacetylase among bacteria (Landry et al., 2000; Tsang and Escalante-Semerena, 1998). It removes the acetyl group from acetyl-lysines, utilizing NAD+ and producing nicotinamide (NAM) and 2”-O-acetyl-ADP-ribose as byproducts. CobB is also the only sirtuin-like deacetylase identified in *E. coli* so far (Zhao et al., 2004). Its activity regulates global protein acetylation level (Castaño Cerezo et al., 2014; Choudhary et al., 2014; Kuhn et al., 2014; Weinert et al., 2017, 2013) and thus affects many cellular functions, including gene expression (Lima et al., 2011; Qin et al., 2016; Thao et al., 2010), the cell cycle (Zhang et al., 2016), metabolism (Castaño Cerezo et al., 2014; Castaño-Cerezo et al., 2011; Venkat et al., 2017), stress response (Castaño Cerezo et al., 2014; Hu et al., 2013; Ma and Wood, 2011), motility and pathogenicity (Liu et al., 2018). In addition, CobB can also act as desuccinylase, de-2-hydroxyisobutyrylase and lipoamidase (Colak et al., 2013; Dong et al., 2019; Rowland et al., 2017). Despite its important role, factors affecting protein deacetylation rate in bacteria are poorly understood. The levels of CobB reaction product NAM (Gallego-Jara et al., 2017), as well as NADH and c-di-GMP (Xu et al., n.d.) have been implicated in regulation of CobB activity so far.

In eukaryotic cells, interplay between activity of sirtuins and NAD+ metabolism is well established, showing that NAD+ is a crucial factor in controlling chromatin structure, DNA repair, lifespan and circadian rhythm (Imai and Guarente, 2016; James Theoga Raj and Lin, 2019). This makes NAD+ not only an enzyme cofactor in various redox reactions but also an important signaling molecule. Bacterial sirtuins on the other hand, have low K_m’s for NAD+

whereas its intracellular concentration is high (Guan et al., 2014). This may jointly result in lower sensitivity of bacterial sirtuins to regulation by NAD+ than their eukaryotic homologues. *In vivo*, the level of NAD+ is maintained by *de novo* synthesis and salvage pathways (Fig. 1). Both pathways require the pivotal metabolite phosphoribosyl pyrophosphate (PRPP) that is produced by the evolutionary conserved PRPP synthase – Prs (Gazzaniga et al., 2009).

In this work we propose that coordination between NAD+ metabolism and protein acetylation is exerted in *E.coli* by crosstalk of the CobB deacetylase with the PRPP synthase Prs. Namely, we provide evidence that CobB forms a stable complex with Prs which enhances its acetylase activity. Moreover, Prs lysine acetylation at positions K182 and K231 can be regulated by CobB and in turn - affects CobB function *in vivo.* This renders CobB-mediated proteome deacetylation dependent on the status of Prs acetylable lysine residues in *E. coli* cells. Consequently – acetylation of Prs affects physiological processes dependent on protein acetylation in *E. coli* – acetate consumption and glycolysis. We propose a model encompassing the interplay of Prs and CobB in regulation of metabolic processes with respect to NAD+ demand.

Results

CobB interacts with phosphoribosyl phosphate synthase *in vivo* and *in vitro*. Numerous acetylated proteins have been suggested to be CobB targets *in vivo*. Some of them were found in global acetylome studies showing differential acetylation of proteins in wild-type and *ΔcobB* mutants (Castaño Cerezo et al., 2014; Weinert et al., 2017). Others were identified as CobB interactants with the use of a protein microarray consisting of the majority of the *E.*

coli proteome (~4000 protein, non-acetylated) (Liu et al., 2014). In order to investigate the regulation of CobB-mediated protein deacetylation we first aimed to identify its interaction partners under physiologically relevant conditions. For this, we performed an immunoprecipitation pull-down, dubbed sequential peptide affinity purification (SPA) (Babu et al., 2009). In this approach, proteins are labeled with a double-affinity tag consisting of triple FLAG epitope and calmodulin binding protein (CBP), separated by a protease cleavage site. After immunoprecipitation from cell lysates with anti-FLAG antibodies, protein complexes are released from the resin by protease digest and re-purified using a calmodulin sepharose column. As a bait, we used chromosomally expressed (from the native promoter), C-terminally SPA-tagged CobB. Subsequently to the pull-down, interaction partners were identified by liquid chromatography coupled to tandem mass spectrometry (LC-MS/MS). The experiments have been carried out using cells grown to stationary phase in a rich undefined medium (LB) and minimal medium containing acetate as a carbon source, both conditions supporting high protein acetylation level. Under those conditions, the major component of the purified CobB complex was the phosphoribosyl phosphate synthase Prs (Supplementary Table 1). This interaction has been previously described by others in a large-scale study of protein-protein interactions, confirming validity of our results (Butland et al., 2005). We further compared our data with the interactions previously described in a CobB protein microarray study (Liu et al., 2014). We found the fatty acids synthesis proteins FabB and FabG are significantly enriched in the presence of CobB, in comparison to control samples analyzed by LC-MS/MS. However, other interactants found in this protein microarray-based investigation were not present or enriched in our data set, suggesting that those interactions are of lower affinity or more transient than the one between CobB and Prs (Supplementary Table 1).

We further confirmed the Prs and CobB interaction performing the pull-down experiment in a reversed set-up, where SPA-tagged Prs was used as a bait (Supplementary Table 1). Consistently, we also observed binding of purified His-tagged Prs (bait) and CobB (prey) in a pull-down experiment (Fig. 2A).

Overall, these results indicate that CobB forms a stable complex with Prs and that the interaction with Prs is one of the most prominent protein-protein interactions formed by CobB in *E. coli* cells.

Prs acetylation state affects *E. coli* physiology and can be regulated by CobB . Next, we asked what function the Prs-CobB complex formation plays in *E. coli* physiology and how it affects biochemical activity of both proteins. Prs has been previously reported as one of the proteins acetylated *in vivo* at widely-conserved positions K182, K194, K231 (Castaño Cerezo et al., 2014; Kuhn et al., 2014; Weinert et al., 2017) (Supplementary figure 1). The role of those modifications for Prs activity has not been clarified. Thus, one possibility for Prs-CobB complex function would be to regulate Prs acetylation state by CobB. Therefore, we asked whether Prs acetylation affects its enzymatic activity and if acetylated Prs is a substrate for CobB deacetylase. To answer the former question, Prs was acetylated non-enzymatically *in vitro* with acetyl phosphate (AcP), as described before by others (Kuhn et al., 2014; Qin et al., 2016). Subsequently, successful modification of lysine residues was confirmed by western blot (Fig. 2B). In addition, we verified by mass spectrometry that the lysine residues of Prs acetylated by AcP are mainly those that had been previously proven to undergo such modification *in vivo* (K182, K194, K231)(Table 1). The most reactive to AcP under conditions used was K182 (Table 1). Next, we measured the influence of Prs lysine acetylation on PRPP formation *in vitro*. However, AcP-mediated acetylation had minor effect on Prs biochemical activity (Fig. 2C). Therefore, we expected

that acetylation status of Prs, especially at position K182, may not be linked only to PRPP synthesis rate *in vivo*. To assess physiological importance of Prs lysine-acetylation, we constructed mutants, expressing chromosomal *prs* variants that mimic protein acetylation at the surface-exposed positions 182 and 231 (Prs K182Q and K231Q), or their non-acetylated state (Prs K182R and K231R). We tested how those mutations affect physiology of *E. coli* cells under conditions relevant for protein acetylation-dependent regulation, namely during glycolysis or gluconeogenetic assimilation of acetate. We measured growth of the respective strains in a minimal medium with acetate or glucose as carbon source (Fig. 2D). Interestingly, strains producing Prs K182R or K231R grew slower on acetate than the wild-type strain and their counterparts with Prs K182Q or K231Q variants. The opposite situation was found during bacterial growth in minimal medium supplemented with glucose. In this case, strains producing Prs K182R or K231R reached an higher OD faster than the wild-type strain and the strains encoding respective Prs acetyl-lysine mimic variants (Fig. 2D). Those results strongly suggest that lysine acetylation at positions 182 and 231 of Prs is physiologically relevant and plays a regulatory role under different metabolic regimes. Weak impact of acetylation on Prs enzymatic activity *in vitro* implies that modification of those lysines may regulate also other Prs function than that of PRPP synthase. Moreover, non-enzymatically acetylated Prs was effectively deacetylated by CobB *in vitro* (Fig. 2E Table 1), confirming that Prs can be CobB substrate.

We further investigated whether Prs interaction with CobB is affected by acetylation of its lysine residues. To achieve this, we repeated the pull-down experiment using acetylated His-tagged Prs and CobB. Non-enzymatically acetylated Prs interacted with CobB in a manner indistinguishable from the unmodified protein (Fig. 2F). It is worth noting that the pull-down reactions did not contain NAD+, disabling deacetylation of Prs by CobB during the course of reaction. Our experiments revealed also that CobB likewise becomes acetylated by acetyl

phosphate in a system consisting of purified proteins (Fig. 2E) and acetylation has moderate influence on its deacetylase activity (Fig. 2D). Acetylated lysine residues of the sirtuin were subsequently identified by MS and are presented in Supplementary table 2. Moreover, our result also showed that CobB undergoes auto-deacetylation *in vitro* (Fig. 2D, Supplementary table 1). It remains unknown if CobB acetylation is of physiological importance. However, neither Prs nor CobB acetylation had any impact on their protein-protein interaction compared to the non-acetylated protein (Fig. 2EF). This suggests that acetylated lysine residues in Prs do not take part in its physical interaction with the CobB deacetylase. We further probed this by repeating the pull downs with purified Prs variants where the acetylable lysines K182, K194 and K231 were substituted by alanines. All three variants were still able to interact with CobB (Fig. 2F). Corroborating those results, we found that CobB was efficiently pulled-down by Prs in *ΔpatZ* and *Δpta* strains (Supplementary table 1). The former strain is devoid of protein lysine acetyltranferase PatZ (Ma and Wood, 2011), the latter lacks phosphate acetylase (Wolfe, 2005) which synthesizes acetyl phosphate. The two strains are characterized by decreased level of enzymatic and non-enzymatic acetylation, respectively (Schilling et al., 2015; Weinert et al., 2013). We next asked, whether assembly with CobB influences non-acetylated Prs activity. Prs synthesizes PRPP from ribose 5-phosphate and ATP, producing AMP as a byproduct (Hove-Jensen et al., 2017). It utilizes magnesium and phosphate ions as a cofactor and allosteric activator, respectively (Willemoes et al., 2000). To assess Prs catalytic activity, we monitored AMP formation using a luciferase based assay that produces a luminescent signal proportional to AMP present in the samples.

Results of this assay showed that addition of CobB alone, CobB together with its substrate NAD+ or product NAM had little impact on Prs activity, when sufficient amount of magnesium and phosphate ions was provided (Supplementary figure 2). Conversely, when assays were carried out under conditions of low magnesium or phosphate concentration,

CobB significantly stimulated Prs activity (Fig. 2G). The intracellular magnesium level has been previously implicated as one of the factors regulating protein acetylation in *E. coli* cells. Namely, protein acetylation was higher in cells grown in magnesium-limited media(Christensen et al., 2017), which could be attributed to Prs activity and NAD+ synthesis. Interaction with CobB also slightly enhanced feedback inhibition of Prs activity by PRPP (Fig. 2H). This suggests that under optimal conditions for the Prs function, assembly with CobB has little influence on non-acetylated Prs enzymatic activity, but CobB may balance PRPP synthesis by Prs under certain physiological conditions.

In summary, our results have shown that Prs and CobB form a complex and their interaction does not rely on Prs acetylation or acetylable lysine residues of Prs. However, Prs is a substrate for CobB *in vitro*, whereas lysine acetylation state (K182 and K231) exerts physiological effect on *E. coli* growth on different carbon sources. Though, acetylation, at least at position K182, has little influence on Prs activity as PRPP synthase.

CobB activity and proteome acetylation is affected by Prs K182 and K231 acetylation status. Both gluconeogenetic metabolism during growth on acetate and glycolysis during growth on glucose-containing media, are regulated by acetylation of the respective metabolic enzymes (Wang et al., 2010). The reciprocal influence of Prs variants mimicking acetylation or non-acetylated state during growth on gluconeogenetic and glycolytic substrates, together with Prs-CobB complex formation, led us to speculate that Prs may influence CobB activity and that the effect might be mitigated by Prs acetylation. Corroborating this hypothesis, we found that the mutations in the *prs* gene, affecting acetylation of the PRPP synthase,as described above, result in profound changes in the global proteome acetylation level. To assess those alterations, we measured protein acetylation in *E. coli* cells, using Western blot and anti-N(ε)-acetyl lysine antibody. Cells were sampled after 12h growth in acetate medium,

when overall acetylation level is high (Schilling et al., 2015; Weinert et al., 2013). In those experiments, cells that chromosomally express *prs* variants K182R and K231R showed higher protein acetylation level than their K182Q and K231Q counterpart (Fig. 3A). This could suggest that CobB deacetylase activity is higher in the mutants that mimic acetylation state (Q) than in acetylation-ablative mutants (R). To further test this hypothesis, we used a system based on fluorescent reporter protein with genetically-encoded acetylated lysine, whose efficiency of fluorescence emission is deacetylation-dependent, and allows to assess deacetylase activity *in vivo* (Xuan et al., 2017). Consistently with the results of protein acetylation assessment by Western blot, we have shown that reporter deacetylation is higher in strains producing Prs variants K182Q and K231Q than in otherwise identical strains producing Prs K182R and K231R (Fig. 3B). Since Prs produces a precursor for NAD+ synthesis, changes in the enzyme's activity could affect intracellular NAD+ concentration, ultimately leading to differences in CobB-mediated protein deacetylation rate. Therefore, to exclude that the introduced amino acid alterations in Prs affect cellular NAD+ pool, we measured NAD+ nucleotide level *in vivo* during exponential growth of bacteria in LB medium. Under those conditions global acetylation level is low and thus, acetylation of the wild-type Prs variant should also be low. All of the changes mimicking lysine acetylation state of Prs had an effect on the cellular NAD+ level. However, in each case, intracellular NAD+ content was increased in comparison to the wild-type strain. This result implies that decreased CobB-mediated protein deacetylation, observed in the strains producing Prs K182R or Prs K231R, is not due to lower CobB activity, resulting from limitation of its substrate (Fig. 3C). Next, we investigated the consequences of complex formation between Prs and CobB on their catalytic activity. First, we tested the effect of Prs-CobB assembly on CobB-mediated removal of acetyl groups from modified lysines. To elucidate this, we measured deacetylation rate of an artificial fluorogenic substrate for Zn2+ and NAD+

dependent deacetylases – MAL (BOC-Ac-Lys-AMC)(Heltweg et al., 2003). In presence of Prs, CobB activity in deacetylating MAL was stimulated by about 50% (Fig. 3D). The degree of stimulation was dependent on Prs concentration and reached maximum in 6:1 molar ratio of Prs to CobB (Prs monomer : CobB monomer) (Supplemetary figure 3). A further increase of Prs concentration had no effect on CobB activity, suggesting that Prs hexamers stimulate a single catalytic center of CobB. As expected, CobB deacetylase activity was dependent on NAD+ concentration and Prs enhanced it in a wide range of NAD+ concentrations, even in those lower than the physiological ones (Bennett et al., 2009) (Fig. 3D). Neither Prs substrates (ribose 5-phosphate, ATP) nor the products of its catalytic activity (PRPP, AMP) and allosteric inhibitor ADP, had significant impact on its biding to CobB or ameliorating deacetylation of MAL substrate (Supplementary figure 4). CobB, as other sirtuins, was proven sensitive to feedback inhibition by deacetylation reaction byproduct – nicotinamide (NAM), with IC_{50} value estimated at approximately 52 μM (Gallego-Jara et al., 2017) (Fig. 3E). NAM is also one of the metabolites of the *E. coli* NAD+ salvage pathway I and its intracellular level has been shown to fluctuate dependent on bacterial growth conditions (Gallego-Jara et al., 2017). This makes NAM a likely candidate for a regulator of CobB activity *in vivo*. Therefore, we tested how the interaction with Prs affects NAM-mediated inhibition of CobB deacetylase activity. In presence of Prs, deacetylation of MAL substrate by CobB was more effective even at very high NAM concentrations, indicating that Prs partially protects CobB from inhibition by NAM (Fig. 3E). We also confirmed using pull-down assay that CobB forms a complex with Prs in the presence of NAM (Supplementary figure 4).

Moreover, it has been shown previously that several metabolites of the NAD salvage pathways, like nicotinamide mononucleotide (NMN), can act as weak inhibitors of Sir2 family deacetylases *in vitro* (Schmidt et al., 2004). Corroborating those results, we observed

that NMN, as well as nicotinic acid adenine dinucleotide (NaAD), NADH and NADP negatively influence CobB activity at high concentrations (Fig. 3D, Supplementary figure 5). As in the case of NAM, Prs increased CobB activity in the presence of those metabolites (Fig. 3D, Supplementary figure 5).

Those results suggest that Prs-CobB interaction influences catalytic activity of CobB by increasing its efficiency as deacetylase. Formation of the complex with Prs also partially protects CobB from inhibition by NAM and other NAD+ metabolites, further suggesting that the interaction exerts an impact on the catalytic center of CobB.

In summary, the results presented so far strongly suggest that formation of the Prs-CobB complex impacts the rate of acetyl group removal from acetylated lysine residues of CobB substrates.

NAD+ is a key cofactor for many enzymes, including glycolytic enzyme GapA and pyruvate dehydrogenase complex. Therefore, NAD+ availability is important to maintain glycolysis rate. Considering differential influence of acetylation state-mimicking alterations in Prs on the growth of *E. coli* strains under glycolytic and gluconeogenetic metabolic regimes, we speculated that Prs acetylation may regulate CobB activity in accordance with NAD+ demand of the main central carbon metabolism pathways. It has been demonstrated that in eukaryotic cells, NAD+-consuming enzymes, including sirtuins, substantially contribute to NAD+ expenditure and impact NAD homeostasis (Strømland et al., 2019). This relationship in *E. coli* has not been investigated, whereas its existence would support the need of coupling between deacetylation and NAD+ biosynthesis and explain the purpose of Prs-CobB complex formation. Therefore, we were interested whether the absence of CobB function will influence the level of NAD+ metabolites. We employed metabolomics to quantitatively assess the intracellular levels of those compounds in wild-type and *ΔcobB* strains. Indeed, we observed that in absence of CobB, concentration of all metabolites of the

NAD synthesis and salvage pathways were raised by about 25% (Fig. 3E), suggesting that CobB is an important player in NAD+ turnover, either by direct NAD+ consumption or regulation of other NAD+ consuming or synthesizing enzymes.

Discussion

In this work we have provided evidence that the CobB deacetylase and the PRPP synthase form a complex in *E. coli*. (Supplementary Table 1, Fig. 2A) Within this complex, both proteins can affect each other's activity (Fig. 2G, 3DE). Why would cells need such an ally? Lysine acetylation is a protein modification that affects protein activity. It allows cells to quickly adjust activity of certain proteins in response to environmental cues, avoiding energy consuming degradation and synthesis. To be efficient as a fast, adaptable regulatory system, acetylation of needs to be reversible at least for some proteins. This is provided by the action of deacetylases, which in bacteria are mostly NAD+-dependent. This makes NAD+ concentration a possible mean to regulate the rate of protein deacetylation. In eukaryotic cells, a clear link has been shown between sirtuins activity and processes influencing the level of NAD+ and its metabolites, like NAM (Anderson et al., 2017; Imai and Guarente, 2016; Lu and Lin, 2010; Zhang and Sauve, 2018). Bacterial sirtuins have low K_m values for NAD+ and prokaryotic cells lack compartmentalization that could facilitate spatial regulation of NAD+ level. In addition, NADH is a rather weak inhibitor of CobB activity, whereas intracellular NADH concentration is around two orders of magnitude lower than that of NAD+ (Bennett et al., 2009). All those factors may limit the possibility of a direct regulation of CobB activity by NAD+ or NAD/NADH ratio in bacterial cells. Dynamics of NAD+ synthesis under various growth conditions is poorly understood. Nevertheless, NAD+ synthesis *de novo* and through salvage pathways requires nicotinamide moiety, ribose

phosphate, provided by PRPP, and adenine nucleotide. The two latter metabolites both link NAD+ and cellular energetics to Prs.

In this work, we present evidence that Prs and CobB form a complex which affects CobB activity (Fig. 3DE). Moreover, we show that Prs acetylation status at positions K182 and K231 influences CobB-mediated protein lysine deacetylation *in vivo* (Fig. 3AB). This results in differential influence of Prs acetylation/deacetylation on bacterial growth on glucogenic and gluconeogenetic substrates (Fig. 2D). We propose that CobB stimulation by Prs is enhanced *in vivo* when K182 or K231 of Prs are acetylated. Prs acetylation likely increases during growth on acetate due to higher expression of PatZ acetylase upon relieving of catabolite repression(Castaño-Cerezo et al., 2011). In support of this notion, acetylation of Prs decreases in strains devoid of Prs activity (Castaño Cerezo et al., 2014) This would enhance deacetylation by CobB, and hence, increase activity of acetate synthase (Acs) and enzymes of gloxylate pathway, like AceA, both required for efficient growth on acetate and regulated by lysine acetylation in *E. coli* and closely related *Salmonella enterica* (Fig. 4)(Castaño Cerezo et al., 2014; Wang et al., 2010). Such mechanism is consistent with more efficient growth of strains producing acetylation-mimicking Prs variants in comparison to their counterparts containing acetylation-ablative Prs form, during cultivation on acetate. Conversely, during growth on glucose, acetylation of Prs can be lower, due to inhibition of PatZ expression, resulting in lower CobB stimulation. As shown before by others, acetylation of two glycolysis/gluconeogenesis enzymes – GapA and Fbp is increased in *ΔcobB* strains (Castaño Cerezo et al., 2014). In *S. enterica*, GapA acetylation favors flux through towards glycolysis over gluconeogenesis(Wang et al., 2010). Thus, lower CobB stimulation may cause higher GapA acetylation and simultaneously incase available NAD+, both ways stimulating glycolysis (Fig. 4). It is consistent with enhanced growth of strains producing Prs that cannot be acetylated, in media containing glucose.

Moreover, while the *cobB* gene is constitutively expressed (Castaño-Cerezo et al., 2011), *prs* is regulated at transcriptional level and activated by low purine and pyrimidine nucleotides concentration (He et al., 1993; White et al., 1971). Hence, the number of Prs-CobB complexes formed in the cell and the overall CobB deacetylation rate would depend on the demand to synthesize new purine nucleotides, including ATP precursors (see graphical abstract). In line with such mechanism, several purine synthesis enzymes, like PurA and Adk were found among proteins acetylated in *E. coli* cells (Weinert et al., 2013; Zhang et al., 2013). The effect of acetylation on those enzymes has not been determined so far but acetylation has often an inhibitory effect. Thus, transcriptional activation of *prs* could ultimately lead to more effective protein deacetylation by CobB and, among other effects, to an increase in the activity of purine synthesis pathway.

In summary, the crosstalk between Prs and CobB allows *E. coli* cells to integrate various cues and adjust protein acetylation level to metabolism and NAD+ demand.

Methods

Materials, reagents and strains

Primers used in this study were synthesized by Sigma/Merck. List of primers, vectors and strains is available in Supplementary table 3. Polymerases and enzymes used for cloning were purchased from Thermo Scientific or New England Biolabs. Reagents used for buffers were purchased from either Carl Roth or Bioshop Life Science. NAD^+ salvage pathway substrates were purchased from Sigma/Merck except for nicotinamide (NAM) which was purchased from Bioshop Life Science.

Mutagenesis was performed with lambda Red recombineering as described earlier (Baba et al., 2006). Strains with single mutations replacing acetylated lysine for arginine or glutamine in *prs* gene: MG1655:*prs*K182R, MG1655:*prs*K182Q, MG1655:*prs*K231R,

MG1655:*prs*K231Q; and strain with *cobB* deletion MG1655:Δ*cobB;* were constructed by recombineering in MG1655 wild-type strain (Baba et al., 2006). Strain with single mutation in active site of CobB replacing histidine for alanine: MG1655:*cobB*H147A was constructed by recombineering in MG1655:Δ*cobB* strain by introducing the mutated *cobB* allele into its primary locus

Cloning, expression and purification of recombinant proteins

His-Prs and catalytically inactive His-PrsK194A were expressed from pET28a-His-*prs* and pET28a-His-*prs*K194A vectors in *E. coli* Rosetta (DE3) as we described earlier (Walter et al., 2020). Additional point mutations replacing acetylated lysines K182 and K231 for alanines were introduced into pET28a-His-*prs* vector with phosphorylated primers (Walter et al., 2020). *E. coli* Rosetta (DE3) was transformed with pET28a-His-*prs*K231A, grown to OD_{600} between 0.8 and 1.0 and induced with 100 µM Isopropyl β-D-1-thiogalactopyranoside (IPTG) at 37°C for 5 h in 2xYT medium (BioShop). *E. coli* BL21-DE3-pLysE was transformed with pET28A-His-*prs*K182A and induced at OD_{600} between 0.8 and 1.0 with 1 mM IPTG at 37°C for 3 h in 2xYT medium.

The *cobB* sequence, amplified on *E. coli* MG1655 genomic DNA was N-terminally cloned with RF-cloning (Bond and Naus, 2012) into modified pET28a-TEV vector (Walter et al., 2020). The *E. coli* Rosetta (DE3) was transformed with vector pET28a-His-TEV-*cobB*, grown in Terrific Broth (BioShop) to OD_{600} between 0.8 and 1.0 and induced with 200 µM IPTG at 37°C for 5 h.

His-Prs protein and its variants were purified at 20°C, as described earlier (Walter et al., 2020) with buffer A (50 mM potassium phosphate pH 7.5, 10 % glycerol, 500 mM NaCl, 20 mM imidazole pH 7.8); buffer B (50 mM potassium phosphate pH 7.5, 10 % glycerol, 500 mM

NaCl, 300 mM imidazole pH 7.8, 0.5 mM tris(2-carboxyethyl)phosphine (TCEP)) and dialysis SEC1 buffer (50 mM potassium phosphate pH 8.2, 10 % glycerol, 500 mM NaCl). Non-acetylated CobB was purified on His-Trap columns (GE healthcare) as described above however, the lysate was loaded on the column and protein eluted on ice. Further, fractions containing protein were combined and diluted 1:1 with buffer A-0 (50 mM potassium phosphate pH 8.2, 10 % glycerol) and supplemented with Dithiothreitol (DTT) and ethylenediaminetetraacetic acid (EDTA) to a final concentration 1 mM and 0.5 mM respectively. Aliquots of 20 ml were made. TEV protease (0.2 mg) purified in-house[54] was added and incubated at 24 ^{o}C for 3 h with no shaking or rotation. After incubation, NaCl concentration was readjusted to 500 mM by spiking with 5M NaCl stock solution and protein solution was dialyzed overnight into SEC1 buffer at 4°C followed by protein separation from His tag on a His-Trap column (GE Healthcare), concentration with an Amicon Ultra 15 MWCO10kDa (Millipore) filter and size-exclusion chromatography at 4 ^{o}C on a Superdex 200 10/300 GL gel filtration column (GE Healthcare). Purity of the proteins was evaluated on SDS-PAGE gel. Concentrated to 10-15 mg ml^{-1} purified proteins were snap-frozen in liquid nitrogen and stored at -70°C.

Acetylation of His-Prs and CobB proteins during protein purification

His-Prs was purified on His-Trap columns (GE Healthcare) as described above and dialyzed overnight at 20 ^{o}C into 1 x acetylation buffer (100 mM Tris-HCl pH 7.5, 10 % glycerol, 150 mM NaCl) [modified from (Kuhn et al., 2014; Qin et al., 2016)]. Further, it was concentrated using the Amicon Ultra 15 MWCO30kDa (Millipore) filter at 18 ^{o}C to 4 mg ml^{-1} and acetylated with acetyl phosphate (lithium potassium salt, Sigma) at final concentration 20 mM at 24 ^{o}C for 3 h. Following acetylation, His-Prs was concentrated at 18 ^{o}C (Amicon Ultra

15 MWCO30kDa) to approximately 3 – 4 ml and further purified by size-exclusion chromatography at 18 ^{o}C on Superdex 200 10/300 GL gel filtration column (GE Healthcare). His-TEV-CobB, prior to acetylation, was purified and washed on His-Trap columns (GE Healthcare) with buffer Ac (50 mM Tris pH 7.9, 500 mM NaCl, 20 mM imidazole pH 7.8, 10 % glycerol) and eluted on ice with buffer Bc (50 mM Tris pH 7.9, 500 mM NaCl, 300 mM imidazole pH 7.8, 10 % glycerol). Fractions containing protein were combined, diluted 1:1 with buffer A-0 and supplemented with DTT (1 mM), EDTA (0.5 mM) and TEV protease (0.2 mg). Further, fractions were incubated for 3 h at 20°C as above, followed by overnight dialysis at 4°C into acetylation dialysis buffer (100 mM Tris, pH 8.2, 300 mM NaCl, 10 % glycerol). The CobB protein was separated from His tag on His-Trap column (GE Healthcare), concentrated at 4 ^{o}C to 6 mg ml^{-1}, diluted 1 : 1 in 0 x acetylation buffer (100 mM Tris-HCl pH 7.5, 10 % glycerol) and acetylated with acetyl phosphate at final concentration 20 mM at 24 ^{o}C for 3 h. Protein solution was further dialyzed overnight into SEC1 buffer at 4 ^{o}C.

Purity of proteins was evaluated on 10 % SDS-PAGE gel. Purified proteins, concentrated to 10-15 mg ml^{-1}, were snap-frozen in liquid nitrogen and stored at -70°C. Acetylation was evaluated with Western blot probed with anti-acetyl lysine antibodies (1:800 dilution) (Sigma/Merck). Mass spectrometry outsourced to Mass Spectrometry Laboratory IBB PAN, Warsaw, Poland. Two independent batches of both His-PrsAc and CobBAc subjected to acetyl phosphate treatments were purified and acetylation was assessed.

CobB pull-down on His-Prs and its variants.

His-Prs or its variants (10 µg) were bound to 4 µl of Ni-NTA Magnetic Agarose Beads (Qiagen) in 50 µl interaction buffer (50 mM Tris pH 9.0, 30 mM imidazole pH 7.8, 300 mM NaCl, 0.2 % Tween 20, 10 % glycerol) for 1 h on vibrating mixer at 20°C. Following triple

wash with interaction buffer, 30 µg of CobB was added to His-Prs bound to beads in 50 µl fresh interaction buffer and incubated for 2 h on vibrating mixer at 20°C. Beads were washed 4 times with interaction buffer and resuspended in 20 µl 1 x SDS loading dye (31.25 mM Tris pH 6.8, 10 % glycerol, 1 % SDS, bromophenol blue). Proteins were resolved by electrophoresis in 10 % SDS-PAGE gel and visualized with Coomassie Brilliant Blue R250 staining. 4 µg of His-Prs and CobB proteins were loaded on gel separately as control. The experiments were performed in 3 independent repeats and representative gels were shown in figures.

CobB deacetylase activity on MAL (BOC-Ac-Lys-AMC) substrate

CobB deacetylase activity was measured as described earlier (Heltweg et al., 2005, 2003) as deacetylation of MAL substrate (Sigma/Merck), an artificial fluorogenic substrate for Zn^{2+} and NAD^{+} -dependent deacetylases. Briefly, deacetylation of 8 nmol MAL substrate by 320 pmol of CobB was performed for 1 h at 24 ^{o}C in 50 µl sirtuin buffer (50 mM Tris-HCl pH 8.5, 137 mM NaCl, 2.7 mM KCl, 1 mM $MgCl_2$) [modified from (Heltweg et al., 2003)] in presence of NAD^{+} at final concentration 400 µM. The NAD^{+} titration was performed in sirtuin buffer supplemented with NAD^{+} independently at final concentrations 10 µM, 20 µM, 50 µM, 100 µM, 250 µM, 500 µM, 750 µM and 1 mM. The $MgCl_2$ titration was performed in sirtuin buffer containing 400 µM NAD^{+} and $MgCl_2$ was supplemented independently at final concentrations 10 µM, 20 µM, 50 µM, 100 µM, 250 µM, 500 µM, 750 µM, 1 mM, 5 mM and 10 mM. The effect of NAD^{+} salvage pathway substrates was evaluated by adding 5 µl of 50 mM β-nicotinamide mononucleotide (NMN), nicotinamide (NAM), nicotinic acid (NA), nicotinic acid mononucleotide (NaMN), nicotinic acid adenine dinucleotide (NaAD) or 10 mM NADH, NADP, NADPH to the reaction. The effect of Prs influence on CobB activity was measured in sirtuin buffer by addition of 150 pmol, 300 pmol and 600 pmol of Prs

hexamer. The effect of Prs influence on CobB activity in NAD+ titration assay, $MgCl_2$ titration assay and in presence of NAD^+ salvage pathway substrates was measured by addition of 150 pmol of Prs hexamer. All reactions were stopped by addition of 400 µl of 1 M HCl and fluorescent substrate was extracted as an upper phase after vortexing for 30 s with 800 µl ethyl acetate and centrifugation (9 500 x g, 5 min). Ethyl acetate was evaporated under the hood at 65 ^oC and the residue was dissolved in 600 µl acetonitrile buffer (39.6 % acetonitrile, 5 µM KH_2PO_4, 4.6 µM NaOH). The fluorescence (2 x 250 µl) was measured at 330/390 nm in black, flat bottom 96 well plate (Heltweg et al., 2005). The experiments were repeated in at least 3 independent replicates.

CobB deacetylase activity on His-PrsAc

CobB driven deacetylation of His-PrsAc was analyzed by Western blot with anti-acetyl lysine antibodies (Sigma/Merck) and mass spectrometry. Briefly, CobB driven deacetylation of His-PrsAc was performed in sirtuin buffer (as above) for 1 h at 24^oC in the presence of 400 µM NAD^+. Deacetylation of 147 pmol Prs hexamer (30 µg of protein) was performed in 50 µl reaction with 650 pmol or 1940 pmol CobB or CobBAc (20 µg and 60 µg of protein respectively). The reaction was stopped by dilution in 4 x SDS loading dye and 5 minutes incubation at 100^oC. Samples were resolved by electrophoresis in 10 % SDS-PAGE gel in duplicates with one gel visualized with Coomassie Brilliant Blue R250 staining and the other transferred to PVDF membrane, probed with anti-acetyl lysine antibodies (1:800 dilution) and visualized. Selected bands were excised from the gel and outsourced for identification of protein lysine acetylation by mass spectrometry to Mass Spectrometry Laboratory IBB PAN, Warsaw, Poland. The experiments were repeated in at least 3 independent replicas and representative gels are shown in figures.

Measurement of Prs catalytic activity

The activity of Prs and its variants was measured as a luminescence signal from AMP formed during catalytic formation of PRPP from ribose-5-phosphate (60 µM) and ATP (60 µM) for 15 min at 37°C. The assay was carried out with His-Prs protein and its variants His-Prs-K194A, His-Prs-K182A and His-Prs-K231A, in 100 µl $MgCl_2$ rich reaction buffer (50 mM Tris pH 8.0, 100 mM KCl, 13 mM $MgCl_2$, 0.5 mM K-phosphate pH 8.0, 0.5 mM DTT, 0.1 mg mL^{-1} BSA) at final Prs hexamer concentration 7 nM (0.7 pmol of hexamer per reaction, 142.8 ng of protein per reaction).

The catalytic activity of His-Prs protein in the presence of CobB at various $MgCl_2$ and potassium phosphate (pH 8.0) concentrations was measured in 100 µl reaction buffer base (50 mM Tris pH 8.0, 100 mM KCl, 0.5 mM DTT, 0.1 mg mL^{-1} BSA) at final Prs hexamer concentration 7 nM and CobB monomer concentration 40 nM (4 pmol of monomer per reaction, 124 ng of protein per reaction). Reactions were supplemented with 1 mM or 3mM potassium phosphate pH 8.0 and / or 1 mM or 3 mM $MgCl_2$.

The activity of His-Prs in presence of various PRPP concentrations was measured in Prs reaction buffer (50 mM Tris pH 8.0, 100 mM KCl, 1 mM $MgCl_2$, 0.5 mM K-phosphate pH 8.0, 0.5 mM DTT, 0.1 mg ml^{-1} BSA) at final Prs hexamer concentration 7 nM and CobB monomer concentration 40 nM.

Reactions were ceased by placing samples immediately after incubation on iced water. The concentration of AMP was measured with AMP-Glo™ Assay (Promega) according to manufacturer`s protocol. Briefly, the luminescence was measured for 10 µl subsample after adding 10 µl of AMP-Glo™ Reagent I which stopped the reaction, removed remaining ATP (1 h incubation at 24°C) and converted AMP produced into ADP, followed by conversion of ADP to ATP through luciferase reaction with the AMP-Glo™ reagent II (1 h incubation at 24°C). The luminescence was measured in white 96 well plate and the concentration of AMP

in experimental samples was calculated based on AMP standard curve measured in triplicates. The catalytic activity of His-Prs protein variants was measured in two independent repeats while the activity in other conditions was measured in at least 3 independent experiments.

Detection of acetylated proteins *in-vivo*

The acetylation level of the whole *E. coli* proteome was measured in M9 minimal medium (1 x M9 salts, 0.1 mM $CaCl_2$, 2 mM $MgSO_4$, 0.04 % thiamine, 25 g l^{-1} uridine) supplemented with 0.2% sodium acetate in early stationary phase (12 h). Bacterial cells (bacterial culture volume = $12/OD_{600}$) were harvested and the pellet was snap-frozen in liquid nitrogen. Frozen pellet was resuspended in 350 µl lysis buffer (30 mM Tris pH 6.8, 10 % glycerol, 100 mM NaCl, 0.2 mM tris(2-carboxyethyl)phosphine (TCEP), 1 x Pierce Protease inhibitors (ThermoFisher Scientific)) followed by 30 s sonication with 2 s :5 s pulsing : rest with 20 % amplitude in an ice-block. Samples were centrifuged 10 min at 16 000 x g, 4°C and protein concentration was measured with Bradford assay. Samples (7.5 µg) were resolved by electrophoresis in 10 % SDS-PAGE gel in duplicates, with first gel visualized with Coomassie brilliant blue and second transferred to PVDF membrane (80 min, 80 V), blocked in 7 % skimmed milk, probed with anti-acetyl lysine antibodies (1:800 dilution) and visualized. The representative gels and Western blots were repeated in at least 3 independent experiments.

Measurement of CobB activity *in-vivo* with fluorescent probe

CobB activity in *prs* and *cobB* mutant strains was measured by expression of a fluorescent probe from the pULtra-AcKRS-$tRNA^{Pyl}$-EGFP(K85TAG) plasmid described by (Xuan et al., 2017). The amber (TAG) mutation in the EGFP at essential for fluorophore maturation lysine K85 allowed incorporation of acetylated lysine (AcK) present in media with orthogonal

amber suppressor pyrrolysyl-tRNA synthetase mutant (AcKRS)/$tRNA^{Pyl}$ pair specific for AcK. Deacetylation results in formation of a fluorescent EGFP while in the absence of deacetylases the EGFP mutant remains non-fluorescent. The chromosomally-encoded CobB activity was measured in the following strains: MG1655 wt, MG1655:Δ*cobB*, MG1655:*cobB*H147A, MG1655:*prs*K182R, MG1655:*prs*K182Q, MG1655:*prs*K231R and MG1655:*prs*K231Q, freshly transformed with pULtra-AcKRS-$tRNA^{Pyl}$-EGFP(K85TAG) plasmid and plated on LB plate supplemented with 25 mg l^{-1} spectinomycin while MG1655:Δ*cobB* as a negative control was freshly plated on LB agar plate. A single colony was inoculated into 18 mL LB supplemented with 5 mM AcK (N(epsilon)-Acetyl-L-lysine, Alfa Aesar, J64139.03) and 25 mg l^{-1} spectinomycin (except for the negative control MG1655:Δ*cobB* which was incubated in LB supplemented with AcK only). The cultures were grown until OD_{600}=0.5 and induced with 1mM Isopropyl β-D-1-thiogalactopyranoside (IPTG). Bacterial cells (bacterial culture volume = $1/OD_{600}$) were collected at 10 h and 14 h, washed twice in 500 µl of PBS, snap-frozen in liquid nitrogen and stored at -20°C. Further, pellets were thawed and resuspended in 500 µl of PBS and fluorescence was measured (excitation 450 nm; emission 510 nm) for 100 µl sample in a flat bottomed, transparent 96 well plate. The *in-vivo* activity of native CobB protein was measured in at least 3 independent repeats.

Determination of NAD level

Measurement of NAD was assessed using NAD/NADH quantitation kit (Sigma-Aldrich). Briefly, MG1655 wild-type strain and MG1655 *prs* and *cobB* mutant strains were grown in LB medium with aeration at 37°C to OD_{600} ~0.5. Bacterial cells (bacterial culture volume = $15/OD_{600}$) were harvested, 25 ml of ice-cold methanol (-20°C) was added and centrifuged at 10 000 x g for 5 minutes at 0°C. Supernatant was removed, pellets were snap-frozen in liquid

nitrogen and stored at -80°C not exceeding 24 h. Prior to the measurement, cell pellet was resuspended in 250 µl of NADH/NAD extraction buffer, sonicated (30 s sonication with 2 s :5 s pulsing : rest with 20 % amplitude in an ice-block) and centrifuged 5 min at 15 000 x g. Proteins were removed with 10 kDa cut-off spin filters. 50 µl samples were measured according to manufacturer`s instructions. The activity was measured for at least three independent biological repeats.

NAD+ metabolomics

Metabolomics was performed by Creative Proteomics. Briefly, MG1655 strain and its *ΔcobB* strain were grown in LB medium with aeration at 37°C to OD_{600} ~0.3. At this point 1ml of sample was withdrawn, cells pelleted and flash-frozen. For the measurements, the cell samples were thawed on ice and each sample (ca. 25 µL) was added with 25 µL of an internal standard (IS) solution containing isotope-labeled NAD, NADH, NA and NAM. Cells were lysed with the aid of two 3-mm metal balls on a MM400 mill mixer for 1 min at 30 Hz. 75 µL of acetonitrile was then added. After vortexing for 10 s and sonication in an ice-water bath for 30 s, the samples were centrifuged at 4°C to pellet protein. Clear supernatants were collected and the pellets were used for protein assay using a standard BCA procedure (Pierce). Standard solutions: a mixed standard solution containing all the targeted compounds were prepared at 20 nmol/mL in a mixture of IS solution - 50% acetonitrile (1:4). This solution was serially diluted at 1 to 4 (v/v) with the same solution. A Waters Acquity UPLC system coupled to a 4000 QTRAP MS instrument was operated in the mode of multiple-reaction monitoring (MRM)/MS.

Quantitation of NAD, NADH, NADP, NADPH, NaMN, NMN and NA

40 µL of each supernatant or each standard solution was diluted 3 fold with water. 20-µL aliquots of the resulting solutions were injected to run LC-MRM/MS with negative-ion

detection on a C18 column (2.1x100 mm, 1.8μm) and with an ammonium formate buffer (A) and methanol (B) as the mobile phase for gradient elution (efficient gradient 5% to 50% B in 10 min) at 0.3 mL/min and 40°C.

Quantitation of NAM

Mix 25 μL of each supernatant or each standard solution with 4 volumes of 60% acetonitrile. 10 μL aliquots of the resulting solutions were injected to run LC-MRM/MS with positive-ion detection on a HILIC column (2.1x100 mm, 1.7μm) and with the use of 0.1% formic acid (A) and acetonitrile (B) as the mobile phase for gradient elution (efficient gradient 90% to 15% B in 12.5 min) at 0.3 mL/min and 30 ^{o}C.

Analytical Results

Concentrations of detected compounds were calculated from the constructed linear-regression curve of each compound with internal standard calibration using the analyte-to-IS peak ratios measured from sample solutions.

Acknowledgements

The authors thank dr Ian Cadby (University of Birmingham, UK) and Krzysztof Sitko (University of Gdansk) for assistance in some of the presented experiments, and Prof. Peter G. Schultz lab (Scripps Research Institute, La Jolla, USA) for providing plasmid system for measuring *in vivo* sirtuins activity. This work was supported by the National Science Center (Narodowe Centrum Nauki, Poland) [No. UMO-2014/13/B/NZ2/01139 to M.G.] and the University of Gdansk [539-D140-B858-21 and 533-D000-GF53-21 to B.W.; and 533-0C20-GS33-21 to A.S.].

Authors contribution

B.W. performed majority of the experimental work, contributed to work conceptualization and preparation of the manuscript; J.M-O. performed the MS analysis of protein complexes and reviewed the manuscript; A.S. performed a part of the biochemical assays; M.B. contributed to project conceptualization and manuscript writing; A.L. contributed to establishment of protein assays and reviewed the manuscript; M.G. contributed to project conceptualization, data analysis and manuscript writing.

Conflict of interest

The authors declare no conflict of interest

References

Anderson KA, Madsen AS, Olsen CA, Hirschey MD. 2017. Metabolic control by sirtuins and other enzymes that sense NAD+, NADH, or their ratio. *Biochimica et Biophysica Acta (BBA) - Bioenergetics* **1858**:991–998. doi:https://doi.org/10.1016/j.bbabio.2017.09.005

Baba T, Ara T, Hasegawa M, Takai Y, Okumura Y, Baba M, Datsenko KA, Tomita M, Wanner BL, Mori H. 2006. Construction of Escherichia coli K-12 in-frame, single-gene knockout mutants: The Keio collection. *Molecular Systems Biology* **2**. doi:10.1038/msb4100050

Babu M, Butland G, Pogoutse O, Li J, Greenblatt JF, Emili A. 2009. Sequential peptide affinity purification system for the systematic isolation and identification of protein complexes from Escherichia coli. *Methods in molecular biology (Clifton, NJ)* **564**:373–400. doi:10.1007/978-1-60761-157-8_22

Bennett BD, Kimball EH, Gao M, Osterhout R, Van Dien SJ, Rabinowitz JD. 2009. Absolute metabolite concentrations and implied enzyme active site occupancy in Escherichia coli. *Nature Chemical Biology* **5**:593–599. doi:10.1038/nchembio.186

652 Bernal V, Castaño-Cerezo S, Gallego-Jara J, Écija-Conesa A, de Diego T, Iborra JL, Cánovas M. 2014.
653 Regulation of bacterial physiology by lysine acetylation of proteins. *New biotechnology* **31**:586–
654 595. doi:10.1016/j.nbt.2014.03.002

655 Bond SR, Naus CC. 2012. RF-Cloning.org: An online tool for the design of restriction-free cloning
656 projects. *Nucleic Acids Research* **40**:209–213. doi:10.1093/nar/gks396

657 Butland G, Peregrin-Alvarez JM, Li J, Yang W, Yang X, Canadien V, Starostine A, Richards D, Beattie B,
658 Krogan N, Davey M, Parkinson J, Greenblatt J, Emili A. 2005. Interaction network containing
659 conserved and essential protein complexes in Escherichia coli. *Nature* **433**:531–537.
660 doi:10.1038/nature03239

661 Castaño-Cerezo S, Bernal V, Blanco-Catalá J, Iborra JL, Cánovas M. 2011. cAMP-CRP co-ordinates the
662 expression of the protein acetylation pathway with central metabolism in Escherichia coli.
663 *Molecular Microbiology* **82**:1110–1128. doi:10.1111/j.1365-2958.2011.07873.x

664 Castaño-Cerezo S, Bernal V, Post H, Fuhrer T, Cappadona S, Sánchez-Díaz NC, Sauer U, Heck AJ,
665 Altelaar AM, Cánovas M. 2014. Protein acetylation affects acetate metabolism, motility and
666 acid stress response in Escherichia coli . *Molecular Systems Biology* **10**:762.
667 doi:10.15252/msb.20145227

668 Choudhary C, Weinert BT, Nishida Y, Verdin E, Mann M. 2014. The growing landscape of lysine
669 acetylation links metabolism and cell signalling. *Nature Reviews Molecular Cell Biology* **15**:536–
670 550. doi:10.1038/nrm3841

671 Christensen DG, Orr JS, Rao C V, Wolfe AJ. 2017. Increasing Growth Yield and Decreasing Acetylation
672 in Escherichia coli by Optimizing the Carbon-to-Magnesium Ratio in Peptide-Based Media.
673 *Applied and environmental microbiology* **83**. doi:10.1128/AEM.03034-16

674 Christensen DG, Xie X, Basisty N, Byrnes J, McSweeney S, Schilling B, Wolfe AJ. 2019. Post-
675 translational Protein Acetylation: An elegant mechanism for bacteria to dynamically regulate
676 metabolic functions. *Frontiers in Microbiology* **10**:1–22. doi:10.3389/fmicb.2019.01604

677 Colak G, Xie Z, Zhu AY, Dai L, Lu Z, Zhang Y, Wan X, Chen Y, Cha YH, Lin H, Zhao Y, Tan M. 2013.
678 Identification of lysine succinylation substrates and the succinylation regulatory enzyme CobB
679 in escherichia coli. *Molecular and Cellular Proteomics* **12**:3509–3520.
680 doi:10.1074/mcp.M113.031567

681 Dong H, Zhai G, Chen C, Bai X, Tian S, Hu D, Fan E, Zhang K. 2019. Protein lysine de-2-
682 hydroxyisobutyrylation by CobB in prokaryotes. *Science advances* **5**:eaaw6703.
683 doi:10.1126/sciadv.aaw6703

684 Gallego-Jara J, Conesa AÉ, Puente T de D, Terol GL, Díaz MC. 2017. Characterization of CobB kinetics
685 and inhibition by nicotinamide. *PLoS ONE* **12**:1–19. doi:10.1371/journal.pone.0189689

686 Gazzaniga F, Stebbins R, Chang SZ, McPeek MA, Brenner C. 2009. Microbial NAD Metabolism:
687 Lessons from Comparative Genomics. *Microbiology and Molecular Biology Reviews* **73**:529–
688 541. doi:10.1128/mmbr.00042-08

689 Greiss S, Gartner A. 2009. Sirtuin/Sir2 phylogeny, evolutionary considerations and structural
690 conservation. *Molecules and cells* **28**:407–415. doi:10.1007/s10059-009-0169-x

691 Guan X, Lin P, Knoll E, Chakrabarti R. 2014. Mechanism of inhibition of the human sirtuin enzyme
692 SIRT3 by nicotinamide: Computational and experimental studies. *PLoS ONE* **9**.
693 doi:10.1371/journal.pone.0107729

694 He B, Choi KY, Zalkin H. 1993. Regulation of Escherichia coli glnB, prsA, and speA by the purine
695 repressor. *Journal of Bacteriology* **175**:3598 LP – 3606. doi:10.1128/jb.175.11.3598-3606.1993

696 Heltweg B, Dequiedt F, Verdin E, Jung M. 2003. Nonisotopic substrate for assaying both human zinc
697 and NAD+-dependent histone deacetylases. *Analytical Biochemistry* **319**:42–48.
698 doi:10.1016/S0003-2697(03)00276-8

699 Heltweg B, Trapp J, Jung M. 2005. In vitro assays for the determination of histone deacetylase
700 activity. *Methods* **36**:332–337. doi:10.1016/j.ymeth.2005.03.003

701 Hove-Jensen B, Andersen KR, Kilstrup M, Martinussen J, Switzer RL, Willemoes M. 2017.
702 Phosphoribosyl Diphosphate (PRPP): Biosynthesis, Enzymology, Utilization, and Metabolic
703 Significance. *Microbiology and molecular biology reviews: MMBR* **81**.
704 doi:10.1128/MMBR.00040-16

705 Hu LI, Chi BK, Kuhn ML, Filippova E v., Walker-Peddakotla AJ, Bäsell K, Becher D, Anderson WF,
706 Antelmann H, Wolfe AJ. 2013. Acetylation of the response regulator RcsB controls transcription
707 from a small RNA promoter. *Journal of Bacteriology* **195**:4174–4186. doi:10.1128/JB.00383-13

708 Imai S, Guarente L. 2010. Ten years of NAD-dependent SIR2 family deacetylases: implications for
709 metabolic diseases. *Trends in pharmacological sciences* **31**:212–220.
710 doi:10.1016/j.tips.2010.02.003

711 Imai SI, Guarente L. 2016. It takes two to tango: Nad+ and sirtuins in aging/longevity control. *npj*
712 *Aging and Mechanisms of Disease* **2**:1–6. doi:10.1038/npjamd.2016.17

713 James Theoga Raj C, Lin SJ. 2019. Cross-talk in NAD+ metabolism: insights from Saccharomyces
714 cerevisiae. *Current Genetics* **65**:1113–1119. doi:10.1007/s00294-019-00972-0

715 Kuhn ML, Zemaitaitis B, Hu LI, Sahu A, Sorensen D, Minasov G, Lima BP, Scholle M, Mrksich M,
716 Anderson WF, Gibson BW, Schilling B, Wolfe AJ. 2014. Structural, kinetic and proteomic
717 characterization of acetyl phosphate-dependent bacterial protein acetylation. *PLoS ONE* **9**.
718 doi:10.1371/journal.pone.0094816

719 Landry J, Sutton A, Tafrov ST, Heller RC, Stebbins J, Pillus L, Sternglanz R. 2000. The silencing protein
720 SIR2 and its homologs are NAD-dependent protein deacetylases. *Proceedings of the National*

721 *Academy of Sciences of the United States of America* **97**:5807–5811.
722 doi:10.1073/pnas.110148297

723 Lima BP, Antelmann H, Gronau K, Chi BK, Becher D, Brinsmade SR, Wolfe AJ. 2011. Involvement of
724 protein acetylation in glucose-induced transcription of a stress-responsive promoter. *Molecular*
725 *Microbiology* **81**:1190–1204. doi:10.1111/j.1365-2958.2011.07742.x

726 Liu CX, Wu FL, Jiang HW, He X, Guo SJ, Tao SC. 2014. Global identification of CobB interactors by an
727 Escherichia coli proteome microarray. *Acta Biochimica et Biophysica Sinica* **46**:548–555.
728 doi:10.1093/abbs/gmu038

729 Liu W, Tan Y, Cao S, Zhao H, Fang H, Yang X, Wang T, Zhou Y, Yan Y, Han Y, Song Y, Bi Y, Wang X, Yang
730 R, Du Z. 2018. Protein Acetylation Mediated by YfiQ and CobB Is Involved in the Virulence and
731 Stress Response of <span class="named-content genus-species"
732 id="named-content-1">Yersinia pestis *Infection and Immunity*
733 **86**:e00224-18. doi:10.1128/IAI.00224-18

734 Lu SP, Lin SJ. 2010. Regulation of yeast sirtuins by NAD+ metabolism and calorie restriction.
735 *Biochimica et Biophysica Acta - Proteins and Proteomics* **1804**:1567–1575.
736 doi:10.1016/j.bbapap.2009.09.030

737 Ma Q, Wood TK. 2011. Protein acetylation in prokaryotes increases stress resistance. *Biochemical*
738 *and Biophysical Research Communications* **410**:846–851.
739 doi:https://doi.org/10.1016/j.bbrc.2011.06.076

740 Qin R, Sang Y, Ren J, Zhang Q, Li S, Cui Z, Yao Y-F. 2016. The Bacterial Two-Hybrid System Uncovers
741 the Involvement of Acetylation in Regulating of Lrp Activity in Salmonella Typhimurium .
742 *Frontiers in Microbiology* .

743 Rowland EA, Greco TM, Snowden CK, McCabe AL, Silhavy TJ, Cristea IM. 2017. Sirtuin Lipoamidase
744 Activity Is Conserved in Bacteria as a Regulator of Metabolic Enzyme Complexes. *mBio* **8**.
745 doi:10.1128/mBio.01096-17

746 Schilling B, Christensen D, Davis R, Sahu AK, Hu LI, Walker-Peddakotla A, Sorensen DJ, Zemaitaitis B,
747 Gibson BW, Wolfe AJ. 2015. Protein acetylation dynamics in response to carbon overflow in
748 Escherichia coli. *Molecular Microbiology* **98**:847–863. doi:10.1111/mmi.13161

749 Schmidt MT, Smith BC, Jackson MD, Denu JM. 2004. Coenzyme specificity of Sir2 protein
750 deacetylases. Implications for physiological regulation. *Journal of Biological Chemistry*
751 **279**:40122–40129. doi:10.1074/jbc.M407484200

752 Strømland Ø, Niere M, Nikiforov AA, VanLinden MR, Heiland I, Ziegler M. 2019. Keeping the balance
753 in NAD metabolism. *Biochemical Society transactions* **47**:119–130. doi:10.1042/BST20180417

754 Thao S, Chen CS, Zhu H, Escalante-Semerena JC. 2010. Nε-lysine acetylation of a bacterial
755 transcription factor inhibits its DNA-binding activity. *PLoS ONE* **5**.
756 doi:10.1371/journal.pone.0015123

757 Tsang AW, Escalante-Semerena JC. 1998. CobB, a new member of the SIR2 family of eucaryotic
758 regulatory proteins, is required to compensate for the lack of nicotinate mononucleotide:5,6-
759 dimethylbenzimidazole phosphoribosyltransferase activity in cobT mutants during cobalamin
760 biosynthesis in Sal. *The Journal of biological chemistry* **273**:31788–31794.
761 doi:10.1074/jbc.273.48.31788

762 Venkat S, Gregory C, Sturges J, Gan Q, Fan C. 2017. Studying the Lysine Acetylation of Malate
763 Dehydrogenase. *Journal of molecular biology* **429**:1396–1405. doi:10.1016/j.jmb.2017.03.027

764 Walter BM, Szulc A, Glinkowska MK. 2020. Reliable method for high quality His-tagged and untagged
765 E. coli phosphoribosyl phosphate synthase (Prs) purification. *Protein Expression and Purification*
766 **169**. doi:10.1016/j.pep.2020.105587

767 Wang Q, Zhang Y, Yang C, Xiong H, Lin Y, Yao J, Li H, Xie L, Zhao W, Yao Y, Ning Z bin, Zeng R, Xiong Y,
768 Guan KL, Zhao S, Zhao GP. 2010. Acetylation of metabolic enzymes coordinates carbon source
769 utilization and metabolic flux. *Science* **327**:1004–1007. doi:10.1126/science.1179687

770 Weinert BT, Iesmantavicius V, Wagner SA, Schölz C, Gummesson B, Beli P, Nyström T, Choudhary C.
771 2013. Acetyl-Phosphate is a critical determinant of Lysine Acetylation in E.coli. *Molecular Cell*
772 **51**:265–272. doi:10.1016/j.molcel.2013.06.003

773 Weinert BT, Satpathy S, Hansen BK, Lyon D, Jensen LJ, Choudhary C. 2017. Accurate quantification of
774 site-specific acetylation stoichiometry reveals the impact of Sirtuin deacetylase CobB on the E.
775 coli acetylome. *Molecular and Cellular Proteomics* **16**:759–769. doi:10.1074/mcp.M117.067587

776 White MN, Olszowy J, Switzer RL. 1971. Regulation and mechanism of phosphoribosylpyrophosphate
777 synthetase: repression by end products. *Journal of bacteriology* **108**:122–131.
778 doi:10.1128/JB.108.1.122-131.1971

779 Willemoes M, Hove-Jensen B, Larsen S. 2000. Steady state kinetic model for the binding of
780 substrates and allosteric effectors to Escherichia coli phosphoribosyl-diphosphate synthase.
781 *The Journal of biological chemistry* **275**:35408–35412. doi:10.1074/jbc.M006346200

782 Wolfe AJ. 2005. The acetate switch. *Microbiology and molecular biology reviews: MMBR* **69**:12–50.
783 doi:10.1128/MMBR.69.1.12-50.2005

784 Xu Z, Zhang H, Zhang X, Jiang H, Liu C. n.d. Interplay between the protein deacetylase CobB and
785 second messenger c-di-GMP signaling.

786 Xuan W, Yao A, Schultz PG. 2017. Genetically Encoded Fluorescent Probe for Detecting Sirtuins in
787 Living Cells. *Journal of the American Chemical Society* **139**:12350–12353.
788 doi:10.1021/jacs.7b05725

789 Zhang K, Zheng S, Yang JS, Chen Y, Cheng Z. 2013. Comprehensive Profiling of Protein Lysine
790 Acetylation in Escherichia coli. *Journal of Proteome Research* **12**:844–851.
791 doi:10.1021/pr300912q

Zhang N, Sauve AA. 2018. Regulatory Effects of NAD+ Metabolic Pathways on Sirtuin Activity. *Progress in Molecular Biology and Translational Science* **154**:71–104. doi:10.1016/bs.pmbts.2017.11.012

Zhang Q, Zhou A, Li Shuxian, Ni J, Tao J, Lu J, Wan B, Li Shuai, Zhang J, Zhao S, Zhao GP, Shao F, Yao YF. 2016. Reversible lysine acetylation is involved in DNA replication initiation by regulating activities of initiator DnaA in Escherichia coli. *Scientific Reports* **6**:1–23. doi:10.1038/srep30837

Zhao K, Chai X, Marmorstein R. 2004. Structure and Substrate Binding Properties of cobB, a Sir2 Homolog Protein Deacetylase from Escherichia coli. *Journal of Molecular Biology* **337**:731–741. doi:10.1016/j.jmb.2004.01.060

Figure legends

Figure 1. NAD+ producing and consuming pathways in *E. coli*. NAD+ de novo synthesis from aspartate (thin black arrows) and salvage pathways in *E. coli*:, I (represented jointly by dark and light gray arrows), II (shown by dark gray arrows), IV (from nicotinamide riboside, depicted by thick black arrows). Names of the enzymes engaged in NAD+ metabolism were provided next to the arrows depicting respective reactions. CobB and Prs role in NAD+ transformations is shown. Prs catalyzes PRPP biosynthesis which serves as a substrate for NAD+ formation de-novo from aspartic acid and in NAD+ salvage pathways. NAD+ is essential for CobB mediated protein deacetylation. NAM is a byproduct of this reaction.
NAD - nicotinamide adenine dinucleotide, NMN – nicotinamide mononucleotide; NAM – nicotinamide, NA – nicotinic acid, NAMN - nicotinic acid mononucleotide, NaAD – nicotinate adenine dinucleotide, NR – nicotinamide ribonucleotide, R5P – ribose 5-phospahte, PRPP – phosphoribosyl pyrophosphate, Asp – aspartate

Figure 2. CobB interacts with Prs having some effect on PRPP synthase`s activity in suboptimal conditions

(A) CobB and Prs form a complex *in vitro*. His_6-Prs interacts with CobB in a pull-down assay. His_6-Prs was pre-bound to Ni^{2+}-coated magnetic beads. After washing off the excess of Prs, the beads were incubated with CobB. Unbound protein was removed by washing and the beads were resuspended in a loading dye and separated in 10% SDS-PAGE gel. Lane 3 shows the extent of CobB binding to magnetic beads in the absence of the bait.
(B) Prs and CobB can be acetylated *in vitro* with acetyl phosphate.

Prs and CobB were acetylated in the presence of 20 mM acetyl phosphate and excess of the reagent was dialyzed. Acetylation was confirmed by Western blot with anti-acetyl lysine antibodies.

(C) Acetylation effect on activity of Prs. Acetylated PrsAc exhibits only slightly lower activity in comparison to non-acetylated Prs. Presence of CobB does not significantly influence the PRPP synthase activity.

Prs activity (0.7 pmol) was assessed by measuring AMP formation from ribose 5-phospate (60 μM) and ATP (60 μM) in presence of CobB (4 pmol) in 100 µl reaction buffer (50 mM Tris pH 8.0, 100 mM KCl, 1 mM $MgCl_2$, 0.5 mM K-phosphate pH 8.0, 0.5 mM DTT, 0.1 mg mL^{-1} BSA) After termination of Prs reaction, AMP was converted to ADP and the residual ATP was removed. Next, ATP was produced from ADP and utilized in luciferase reaction. Reactions were performed in 96-well plates and luminescence was measured using plate reader. Mean values of 3 independent experiments were presented. Error bars show SD between the repeats.

(D) Acetyl ablative mutations of Prs decrease growth rate in gluconeogenetic conditions while supporting growth in glycolytic conditions. Growth curve of MG1655 wild-type strain, strains with single mutations in *prs* gene replacing acetyl lysine for arginine (acetylablative) or glutamine (acetyl mimicking), and strain with *cobB* deletion and inactive cobBH147A. Overnight bacterial culture in LB were diluted 1:60 and grown in 96 well plate in final volume 180 µl in a plate reader in M9 Minimal medium supplemented with 0.2 % sodium acetate (M9 ac, left) or 0.2 % glucose (M9 glu, right).

(E) Acetylated Prs (Ac) becomes deacetylated *in vitro* by CobB.

Acetylated Prs and CobB were incubated in the presence of 400 μM NAD+ (1h). Proteins were separated in 10% SDS-PAGE gel and Western blot with anti-acetyl lysine antibodies was subsequently performed. Numbers below the blot image represent the results of densitometric analysis of bands intensity from three independent blots.

(F) CobB interacts with both chemically acetylated Prs and Prs variants with key acetylable lysine residues substituted by alanines. Interaction of acetylated proteins was tested *in vitro* in a pull-down assay, as above. The presence of acetylated protein in a reaction was marked with Ac.

(G) CobB stimulates Prs activity *in vitro* under conditions of low phosphate or magnesium ion concentration.

Prs activity was assessed by measuring AMP formation from ribose 5-phospate (60 μM) and ATP (60 μM). Reaction was performed in the presence of CobB (Prs hexamer : CobB monomer ratio) in 100 µl reaction buffer (50 mM Tris pH 8.0, 100 mM KCl, 0.5 mM DTT, 0.1 mg mL^{-1} BSA) with variable concentration of Mg2+ and PO4- indicated in the figure.

After termination of Prs reaction, the ATP luminescence was measured using plate reader as described above. Mean values of 3 independent experiments were presented. Error bars show SD between the repeats.

(H) CobB slightly increases Prs sensitivity to feedback inhibition by PRPP. Prs activity was measured in 100 µl reaction buffer (50 mM Tris pH 8.0, 100 mM KCl, 1 mM $MgCl_2$, 0.5 mM K-phosphate pH 8.0, 0.5 mM DTT, 0.1 mg mL^{-1} BSA) as described above in the presence of indicated concentrations of PRPP. All measurements were taken in at least 3 independent repeats. Error bars show SD between the repeats.

Figure 3. Prs induces deacetylase activity while its acetylation state orchestrates global acetylation changes.

(A) Prs acetylmimicing variants K182Q and K231Q demonstrate lower global protein acetylation level in comparison to MG1655 wild-type strain and CobB deficient strains. Global protein acetylation was assessed in MG1655 strain and its *cobB* derivatives, producing wild-type Prs or Prs variants K182R, K182Q, K231R and K231Q from the *prs* gene in its native chromosomal position. Overnight cultures of the strains were diluted in M9 medium supplemented with 0.2% sodium acetate and samples were collected after 12 hrs of cell growth. After preparation of whole cell lysates, 7.5 µg of proteins from each of them was separated in 10% SDS-PAGE gel, followed by Western blot with anti-acetyl lysine antibodies.

(B) Strains producing acetylmimicing Prs variants K182Q and K1231Q demonstrated increased CobB activity *in-vivo*.
CobB activity in prs and cobB mutant strains was measured by expression of a fluorescent probe from pULtra-AcKRS-tRNA^{Pyl}-EGFP(K85TAG) plasmid allowing fluorescent EGFP production, activated upon deacetylation. The cultures were grown in LB medium supplemented with acetyl-K and appropriate antibiotics, induced at OD_{600}=0.5 with 1mM Isopropyl β-D-1-thiogalactopyranoside (IPTG) and collected after 10h (light gray bars) and 14h (dark gray bars) since the induction. Fluorescence was measured for 100 µl sample in PBS in a plate reader. Mean values of 3 independent experiments were presented. Error bars show SD between the repeats.

(C) Strains producing Prs acetyl mutants and CobB defective strains demonstrated higher NAD+ level in comparison to the wild-type strain.
NAD+ level was assessed using NAD/NADH quantitation kit (Sigma-Aldrich) according to manufacturer`s description, on samples grown in LB medium with aeration at 37°C, collected in exponential phase at OD_{600}=0.5. Samples were measured with a plate reader according to the manufacturers description. Mean values of 3 independent experiments were presented. Error bars show SD between the repeats.

(D) Prs stimulates CobB activity in a wide range of NAD+ concentrations.
Deacetylation of MAL substrate (8 nmol) by CobB (320 pmol of monomer) in the presence of Prs (300 pmol of hexamer) and indicated amounts of NAD+ was performed for 1h. Fluorescent substrate was extracted with ethyl acetate and fluorescence was measured at 330/390 nm in a plate reader. Error bars represent SD between 3 independent experiments.

(E) Prs partially overcomes inhibition of CobB by NAM.
MAL deacetylation was performed as described above in the presence of indicated amounts of NAM and NMN and Prs (300 pmol of hexamer). Mean values of 3 independent experiments were presented. Error bars show SD between the repeats.

(F) Deletion of the *cobB* gene increases the level of NAD+ metabolites. MG1655 wild-type strain and its *ΔcobB* derivative were grown in LB medium at 37°C with aeration. 1 ml of the cultures was collected at OD_{600} ~0.3 and disrupted in the presence of isotope-labeled standards. Metabolites were extracted with acetonitrile (1:3) and detected with LC-MRM/MS. Concentrations of detected compounds were calculated from the constructed linear-regression curve of each compound with internal standard (IS) calibration using the analyte-to-IS peak ratios measured from sample solutions. Protein concentration was measured with bicinchronic acid kit and protein amount in the sample was taken as proxy of cellular mass present in the sample.

Figure 4. Crosstalk between Prs and CobB in regulation of protein acetylation and metabolism. Proposed metabolic enzyme targets for Prs-CobB control were marked in grey.

Table 1. Acetylated lysines in Prs and their deacetylation by CobB. Chemically acetylated lysines K182, K194, K231 are deacetylated *in-vitro* by CobB deacetylase.
Samples of PrsAc and PrsAc deacetylated by CobB (Fig. 2D) were excised from 2 independent Coomassie stained SDS-Polyacrylamide gels and analyzed with Mass Spectrometry. All identified peptides carrying lysines of interest were summed up (second value in brackets) and acetylated lysines were counted (first value in brackets). The acetylation percentage was calculated and average values are shown in the table. A PrsAc protein sample aliquot was additionally analyzed with mass spectrometry where 108, 82 and 73 peptides with acetylated lysines K182, K194 and K231 respectively were identified suggesting those lysines were acetylated *in-vitro*.

Lysine	Protein sequence	PrsAc		PrsAc after CobB deacetylation	
K182	VVRARAIAKLLNDTDMA	sample1 (6/8)	75%	sample3 (2/34)	6%
		sample2 (16/19)	84%	sample4 (5/54)	9%
		average	80%	average	8%
K194	DTDMAIIDKRRPRANVSQ	sample1 (11/69)	16%	sample3 (3/57)	5%
		sample2 (27/251)	11%	sample4 (0/86)	0%
		average	14%	average	NA
K231	IDTGGTLCKAAEALKERG	sample1 (2/24)	8%	sample3 (0/19)	0%
		sample2 (0/34)	0%	sample4 (0/19)	0%
		average	NA	average	NA

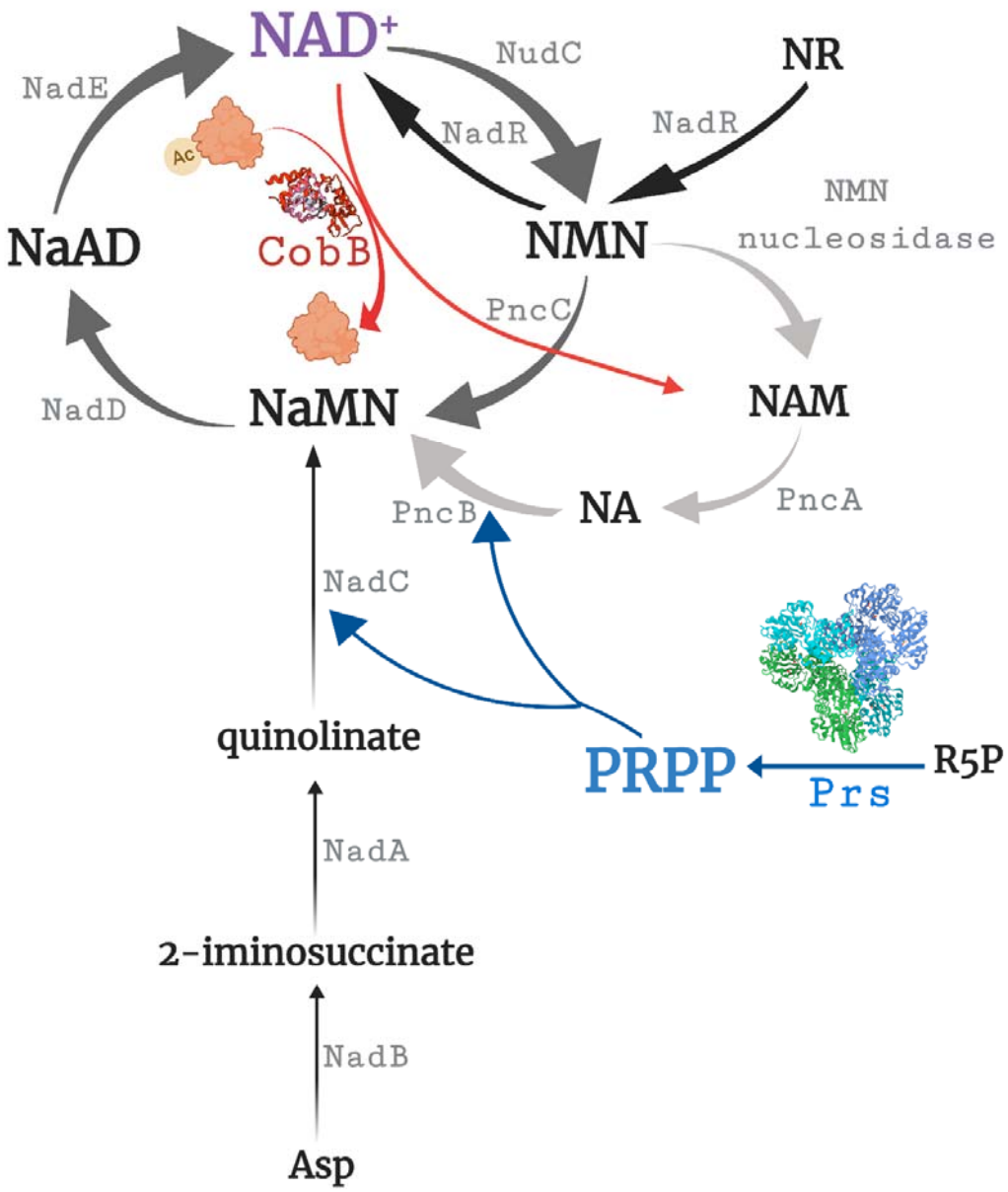
NAD+
NudC
NR
NadE
NadR
NadR
AC
NMN
nucleosidase
NaAD
CobB
NMN
PncC
NadD
NaMN
NAM
PncB
NA
PncA
NadC
quinolinate
PRPP
R5P
Prs
NadA
2-iminosuccinate
NadB
Asp

Fig. 1

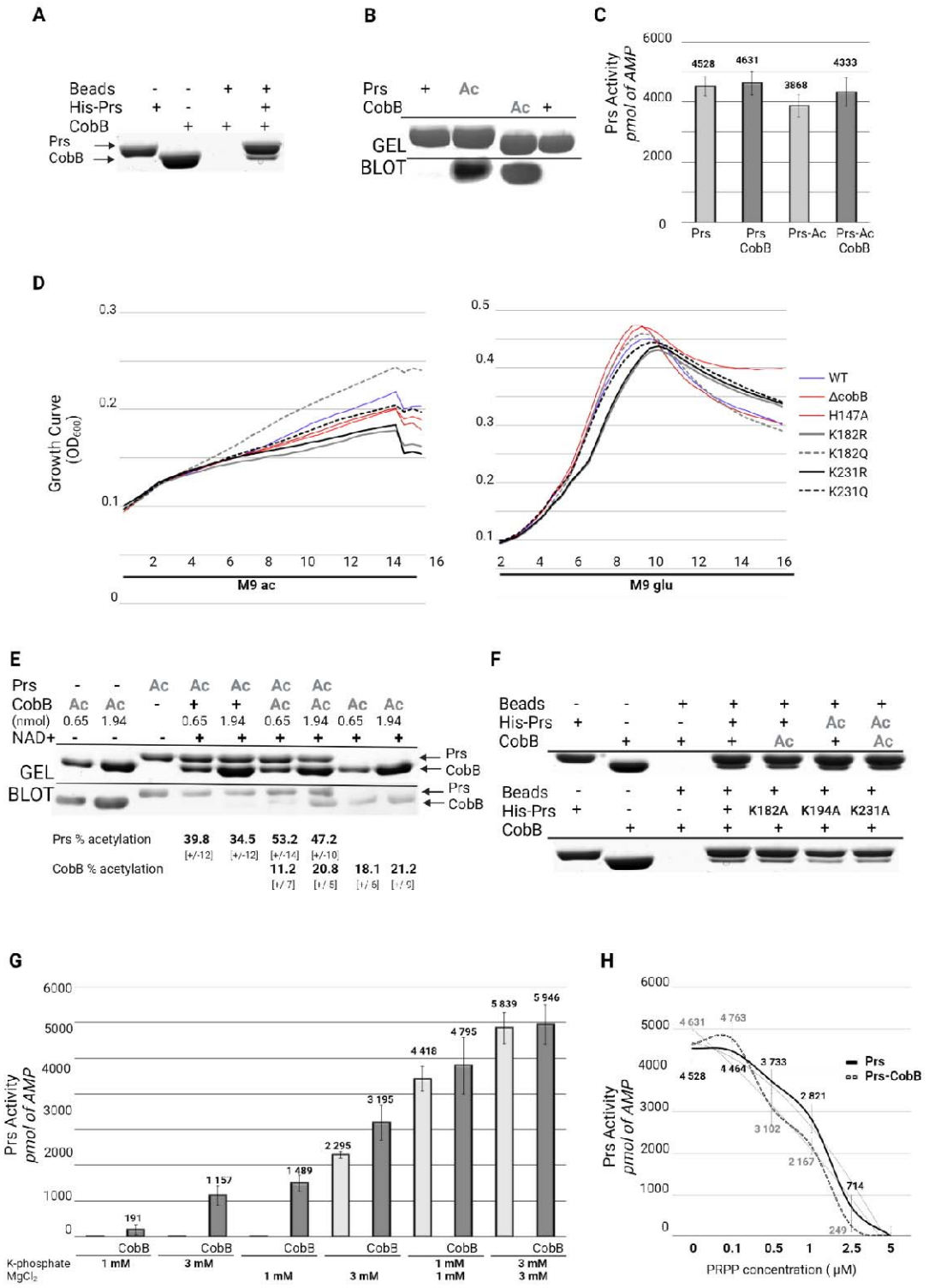
A
Beads - - + +
His-Prs + - +
CobB + + +
Prs
CobB
B
Prs + Ac
CobB Ac +
GEL
BLOT
C
Prs Activity
pmol of AMP
6000
4000
2000
0
4528
4631
3868
4333
Prs
Prs CobB
Prs-Ac
Prs-Ac CobB
D
Growth Curve (OD_{600})
0.3
0.2
0.1
0
2 4 6 8 10 12 14 16
M9 ac
0.5
0.4
0.3
0.2
0.1
2 4 6 8 10 12 14 16
M9 glu
WT
ΔcobB
H147A
K182R
K182Q
K231R
K231Q
E
Prs - - Ac Ac Ac Ac Ac
CobB Ac Ac - + + Ac Ac Ac Ac
(nmol) 0.65 1.94 0.65 1.94 0.65 1.94 0.65 1.94
NAD+ - - - + + + + + +
GEL
BLOT
Prs
CobB
Prs
CobB
Prs % acetylation 39.8 [+/-12] 34.5 [+/-12] 53.2 [+/-14] 47.2 [+/-10]
CobB % acetylation 11.2 [+/-7] 20.8 [+/-5] 18.1 [+/-6] 21.2 [+/-9]
F
Beads - - + + + + +
His-Prs + - - + + Ac Ac
CobB + + + Ac + Ac
Beads - - + + + + +
His-Prs + - - + K182A K194A K231A
CobB + + + + + +
G
Prs Activity
pmol of AMP
6000
5000
4000
3000
2000
1000
0
191
1 157
1 489
2 295
3 195
4 418
4 795
5 839
5 946
CobB
K-phosphate 1 mM 3 mM 1 mM 3 mM 1 mM 1 mM 3 mM 3 mM
$MgCl_2$
H
Prs Activity
pmol of AMP
6000
5000
4000
3000
2000
1000
0
4 631
4 763
4 528
4 464
3 733
2 821
3 102
2 167
714
249
Prs
Prs-CobB
0 0.1 0.5 1 2.5 5
PRPP concentration (μM)

999

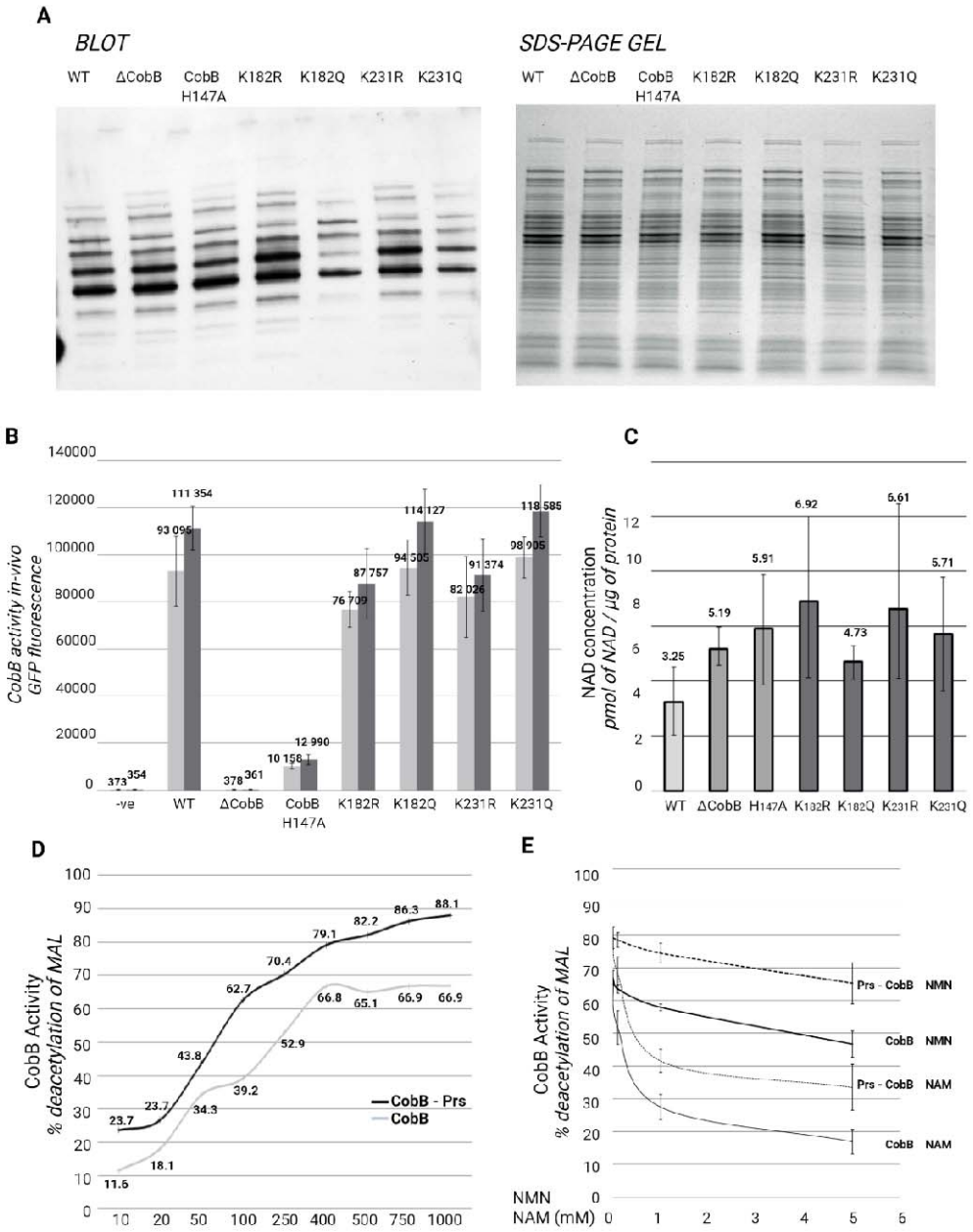
A
BLOT
SDS-PAGE GEL
WT ΔCobB CobB H147A K182R K182Q K231R K231Q
B
CobB activity in-vivo GFP fluorescence
-ve WT ΔCobB CobB H147A K182R K182Q K231R K231Q
C
NAD concentration pmol of NAD / µg of protein
WT ΔCobB H147A K182R K182Q K231R K231Q
D
CobB Activity % deacetylation of MAL
CobB - Prs
CobB
E
CobB Activity % deacetylation of MAL
Prs - CobB NMN
CobB NMN
Prs - CobB NAM
CobB NAM
NMN
NAM (mM)
F
pmol / µg of protein
WT ΔCobB
NA
NAD
NMN
NaAD
NaMN
NADH

1000

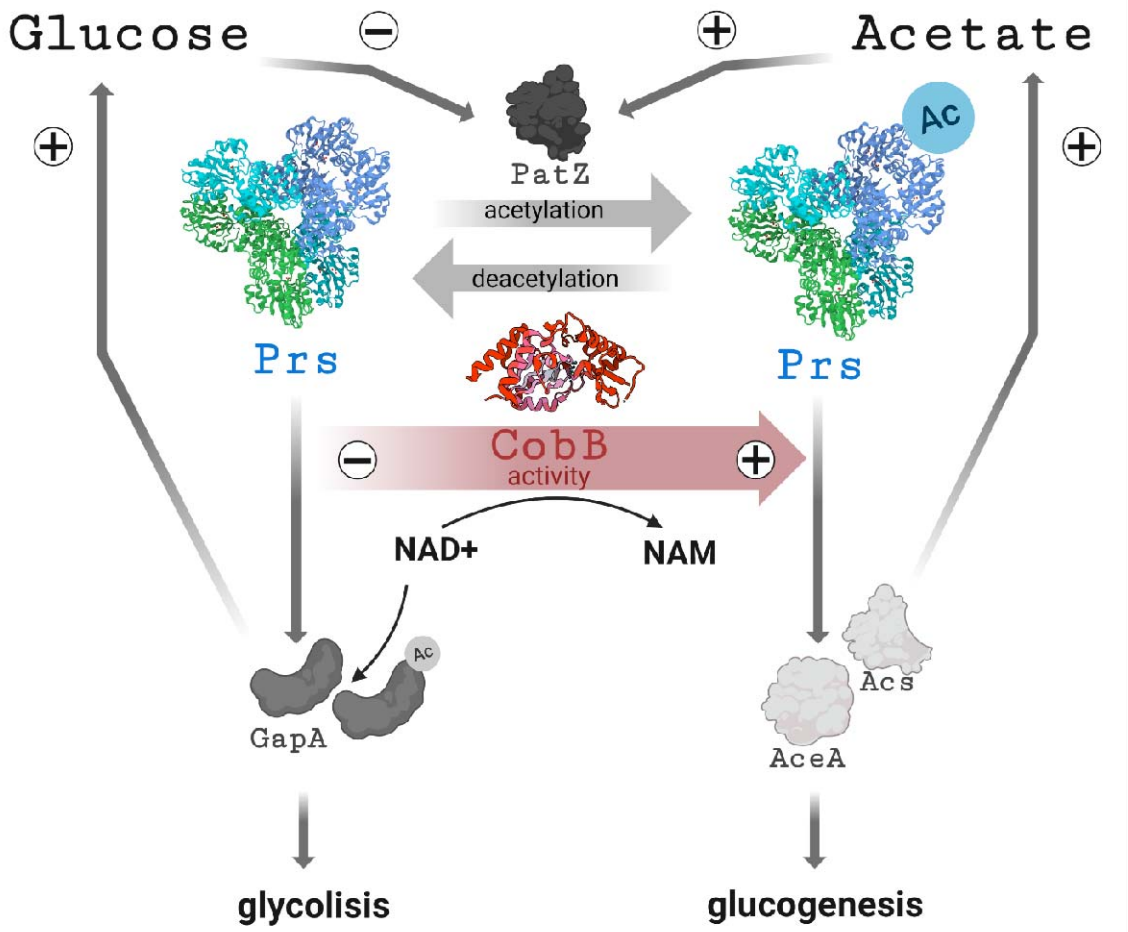
Glucose
Acetate
PatZ
acetylation
deacetylation
Ac
Prs
Prs
CobB
activity
NAD+
NAM
Ac
GapA
Acs
AceA
glycolisis
glucogenesis

Fig 4.

1011